Tikrit Journal of Pure Science Vol. 31 (1) 2026

DOI:https://doi.org/10.25130/tjps.v31i1.1875

IRAQI Academic Scientific Journals

Tikrit Journal of Pure Science

ISSN: 1813 – 1662 (Print) --- E-ISSN: 2415 – 1726 (Online)

Journal Homepage: https://tjpsj.org/

Tikrit Journal of Pure Science

Effect of Immersion Time on Crystallinity and Optical Properties of CdTe Thin Films

Wafaa A. Abdulwahab , Hussein K. Mohammad

Department of Physics, College of Science, University of Tikrit, Tikrit, Iraq

Received: 22 Jan. 2025 **Received in revised forum:** 28 Mar. 2025 **Accepted:** 6 Apr. 2025

Final Proofreading: 28 Jul. 2025 **Available online:** 25 Feb. 2026

ABSTRACT

This study examined the influence of immersion periods in nanoparticles suspension of cadmium telluride (CdTe) prepared by pulsed laser ablation on the structural and optical properties of deposited thin films with a thickness range of 300 to 420 nm. X-ray diffraction (XRD) showed a polycrystalline structure with enhanced crystallinity and an increase in crystallite size from 19 to 21.6 nm with increasing immersion time from 1 to 4 h. Atomic force microscopy (AFM) showed increases in particle diameter and surface roughness with increasing deposition time. These changes were linked with the development of optical absorbance of the deposited films; in addition, the energy gap narrowed from 2.82 to 2.62 eV. Fourier transform infrared spectroscopy (FTIR) confirms the formation of the CdTe structure. These variations make the thin films more suitable for various applications.

***Keywords*:** CdTe nanoparticles, Crystallinity, PLA, Thin films

Name: **Wafaa A. Abdulwahab** **E-mail:** wafaa12.adnan@st.tu.edu.iq

تأثير زمن الغمر على التبلورية والخصائص البصرية لأغشية CdTe الرقيقة

وفاء عدنان عبد الوهاب، حسين خضير محمد

قسم الفيزياء، كلية العلوم، جامعة تكريت، تكريت، العراق

الملخص

تناولت هذه الدراسة تأثير فترات الغمر في محلول الجسيمات النانوية CdTe المحضرة باستخدام تقنية الاستئصال بالليزر النبضي على الخصائص التركيبية والبصرية للأغشية الرقيقة المترسبة بسمك يتراوح ضمن المدى (300 – 420 nm). أظهرت نتائج حيود الأشعة السينية (XRD) بنية متعددة التبلور مع تحسن في التبلور وزيادة في حجم البلورات من (19 nm) الى(21.6 nm) مع زيادة زمن الغمر من ساعة

DOI:https://doi.org/10.25130/tjps.v31i1.1875

واحدة الى 4 ساعات. وأظهرت نتائج مجهر القوة الذرية (AFM) زيادة في قطر الجسيمات وخشونة السطح مع زيادة وقت الترسيب. ارتبطت هذه التغيرات بتحسن في الامتصاص البصري للأغشية المترسبة، بالإضافة الى انخفاض فجوة الطاقة من (2.82 eV) الى (2.62 eV). واكدت نتائج التحليل الطيفي بالأشعة تحت الحمراء (FTIR) تكوين بنية CdTe. هذه التغيرات تجعل الأغشية الرقيقة أكثر ملائمة للاستخدام في تطبيقات مختلفة.

INTRODUCTION

Researchers are interested in metal telluride thin films for their optical and electrical properties, which enable them to be used in a wide range of optoelectronic applications. [1-4]. Cadmium telluride (CdTe) is a direct band gap type II-VI semiconductor that is used in solar cells. [5,6]. CdTe nanoparticles are also utilized in gas sensors and photodetectors. [6,7]. The ability to adjust CdTe characteristics using nanoparticle engineering has made it suitable for application in current technologies. [8]. Pulsed laser ablation (PLA) is a promising technology for preparing nanostructures, as it is highly efficient at producing nanoparticles from high-melting-point solid targets. PLA technique can be controlled by various factors that allow for adjusting the final characteristics of the prepared nanostructures[9,10]. The PLA technique uses high-power, short-pulse laser pulses to interact with the target material, causing sublimation. The ablated material cools, forming nanostructures. [11]. This approach is effective because it can produce pure nanoparticles of regulated size while preserving approximately stoichiometric ratios of the desired components.[12]. Furthermore, many post-deposition procedures can be used to change structural and optical characteristics.[13]. These adjustments can greatly improve the performance of CdTe thin films in certain applications. [14]. This study aims to prepare a CdTe nanofilm by dip-coating from a suspension of CdTe nanoparticles prepared using PLA and to investigate the effects of varying immersion times on the structural, morphological, and optical properties of the resulting thin films.

THEORETICAL ASPECTS

This study explores the fundamental principles of chemical bath deposition (CBD) for CdTe thin-film deposition. It displays the formation and properties of these thin films.

CdTe is a binary semiconductor from the II-VI group, known for its suitability for diverse electronic and optoelectronic applications, particularly in thin-film solar cells. CdTe has an instantaneous band gap of about 1.45 eV. It absorbs most of the incident light within a thin layer. CdTe demonstrates excellent stability across a wide range of environmental conditions, making it suitable for outdoor applications. [15]. CBD is a fee-effective, scalable technique for depositing thin films. It is specifically beneficial for growing uniform CdTe thin films. [16]. Controlled ion launch promotes the nucleation and growth of CdTe crystals, with temperature, pH, and reaction time influencing the film's quality. [17]. Excess ions and by-products are eliminated, leaving a uniform CdTe layer on the substrate. [18]. Several elements affect the structural, optical, and electrical properties of CdTe thin films, including temperature, deposition time, and solution concentration.[19,20].

CdTe's is applied in various applications: photovoltaic devices; where CdTe thin films are extensively utilized in thin-film sun cells due to their excessive efficiency, low value, and compatibility with scalable production, optoelectronic devices; where CdTe thin films are utilized in photodetectors, light-emitting diodes (LEDs), and other optical gadgets, and radiation detectors; where with the excessive atomic number, CdTe is powerful in detecting X-rays and gamma rays. [21].

This has a look at explores the instruction of CdTe skinny films using a hybrid technique that mixes PLA with CBD. PLA produces excessive-purity CdTe nanoparticles suspended in a colloidal

DOI:https://doi.org/10.25130/tjps.v31i1.1875

solution, which serves as the precursor for CBD. The integration of those strategies offers numerous PLA-synthesized nanoparticles with uniform nucleation and growth using the CBD method. By adjusting laser parameters and deposition conditions, the structural and optical properties of CdTe films can be precisely controlled. This combined method offers a price-powerful, scalable approach to producing high-quality CdTe thin films [22].

EXPERIMENTAL

CdTe powder of purity (≥ 99.98 %) supplied from Sigma-Aldrich (3 g) was pressed as a pellet to be used as a target. CdTe nanoparticles suspension was prepared by PLA technique in distilled water using Nd: YAG laser (Diamond-288 EPLS) from CdTe target using (200 pulses) of (600 mJ) laser pulsed energy of (1064 nm) wavelength. Previously cleaned glass slides were used as substrates to immerse in the prepared colloidal suspension of nanoparticles for different periods of time (1, 2, 3, and 4 h). Finally, the slides were dried at room temperature. The prepared CdTe thin films were examined by the XRD technique (SHIMADZU-6000) of (1.54 Å) wavelength at a diffraction angle range from (10° to 80°). AFM was used to characterize the surface morphology of the deposited films. The optical properties were examined by UV-Vis spectroscopy (UV-V Rs 32000 from IndiaMART). The molecular bands were examined using FTIR (SHIMADZU). The thin-film thickness was measured using a spectroscopic reflectometer (TF-Probe from Angstrom Sun Inc.) with a wavelength range of 300 to 420 nm and increasing immersion time from 1 to 4 h.

RESULTS AND DISCUSSION

Figure 1 displays the XRD of the CdTe layers deposited on glass slides at different times (1, 2, 3, and 4 h). The patterns display polycrystalline nature of diffraction lines at 2θ values around (23.8°, 39.4°, 46.5°, 62.5° and 71.3°), corresponding to the Miller indices (111), (220), (311), (331), and (422) of CdTe, which has cubic structure, according to JCPDS card (96-900-8841). Increasing deposition time enhances crystallinity (as shown by the increase in intensity) because more aggregated material promotes additional crystal growth, thereby increasing the film thickness. The preferred orientation along (200) at a (1 h) deposition time corresponds to the (111) direction at a longer deposition time. The (111) plane is typically the most stable low-energy plane. Increasing the thin-film thickness thickens the thin film and relaxes the strain, allowing the thermodynamically preferred (111) orientation to dominate. In addition, the patterns show a decrease in the full width at half-maximum (FWHM) of the diffraction lines, as calculated numerically using the software attached to the XRD device, indicating an increase in crystal size. A minor shift of the peaks' positions towards lower angles indicates a slight change in the lattice dimensions due to the variation in the induced lattice strain with increasing crystallite size.[23].

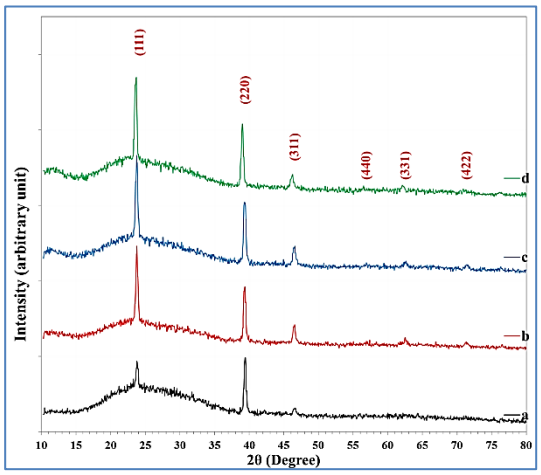

Fig. 1: XRD of CdTe nanoparticles deposited with different times: a=1h, b= 2h, c= 3h, and d=4h.

The inter-planner spacing (d_{hkl}) was determined by Bragg's formula.[24]. The crystallite size was calculated from line broadening using Scherrer's formula. [25]. Table (1) lists the XRD results of diffraction angle (2θ), FWHM, d_{hkl}, crystallite size (D) and Miller indices.

DOI:https://doi.org/10.25130/tjps.v31i1.1875

Table 1: XRD results of CdTe nanoparticles deposited at different periods.

Time (h)	2θ (°)	FWHM (°)	d_{hkl} (Å)	D (nm)	hkl
1	23.8341	0.4276	3.7304	19.0	(111)
	39.4349	0.4944	2.2832	17.1	(220)
	46.5492	0.5555	1.9494	15.6	(311)
2	23.8095	0.4009	3.7341	20.3	(111)
	39.3849	0.4592	2.2860	18.4	(220)
	46.4992	0.4965	1.9514	17.4	(311)
	62.5573	0.6034	1.4836	15.4	(331)
	71.2723	0.6838	1.3221	14.3	(422)
3	23.7579	0.3808	3.7421	21.3	(111)
	39.3332	0.4333	2.2888	19.5	(220)
	46.5238	0.4839	1.9504	17.9	(311)
	62.5311	0.6038	1.4842	15.4	(331)
	71.4748	0.6418	1.3188	15.2	(422)
4	23.7430	0.3766	3.7445	21.6	(111)
	39.1332	0.4313	2.3001	19.5	(220)
	46.3238	0.4692	1.9584	18.4	(311)
	62.3311	0.5880	1.4885	15.8	(331)
	71.2240	0.6398	1.3229	15.3	(422)

The lattice parameter (a) of the cubic form was calculated utilizing the relationship and listed in Table 2. [26]:

$$a = d_{hkl}\sqrt{h^2 + k^2 + l^2} \quad \ldots. \ (1)$$

The lattice parameter increased from 6.4638 Å to 6.4836 Å over 1-4 h, reflecting a decrease in defects and an increase in crystallinity. [27]. The values are comparable to those in previous studies. [28]. Figure 2 compares the crystallite size calculated using the Scherrer formula with the variation in the lattice parameter over the deposition period. A similar trend was observed in both parameters.

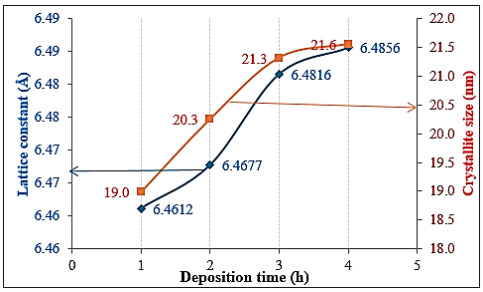

Fig. 2: Variation of crystallite size and lattice constant with deposition time.

AFM analysis of CdTe thin films deposited for different immersion times provides valuable insights into their surface morphology. Figure 3 shows 3D AFM images and particle size distribution plots, highlighting the characteristic changes in surface morphology with changing deposition time. For a sample deposited for 1 h, the AFM image shows irregularly distributed, dispersed particles on the surface. The average diameter of these nanoparticles is 97.32 nm. The low surface roughness of (3.25 nm) indicates a relatively smooth surface texture. The particle size distribution in the accompanying plot shows an irregular distribution due to less deposition on the sample surface.

Increasing the deposition time to 2 h results in a significant increase in the average particle diameter to 101.25 nm. This change indicates increased crystal growth or nanoparticle aggregation, resulting in larger particles. In addition, the surface roughness increases to (4.12 nm) while the particle distribution is homogeneous on the sample surface. Increasing the deposition time to (3 h) increases the average particle diameter to (121.53 nm) while the surface roughness increases to (4.78 nm). In comparison, the sample at (4 h) deposition time had

DOI:https://doi.org/10.25130/tjps.v31i1.1875

a larger particle mass and a larger average size of (125.75 nm) and a surface roughness of (5.67 nm). Table 2 shows the average particle size and surface roughness values for the four samples. The observed differences in surface morphology, particle size and roughness with increasing deposition time are crucial to understanding how the amount of deposited material affects the surface morphology of these nanoparticles and their potential applications. These insights can help determine the optimal conditions and variables to obtain material properties for specific applications, such as photocatalysis or sensing.

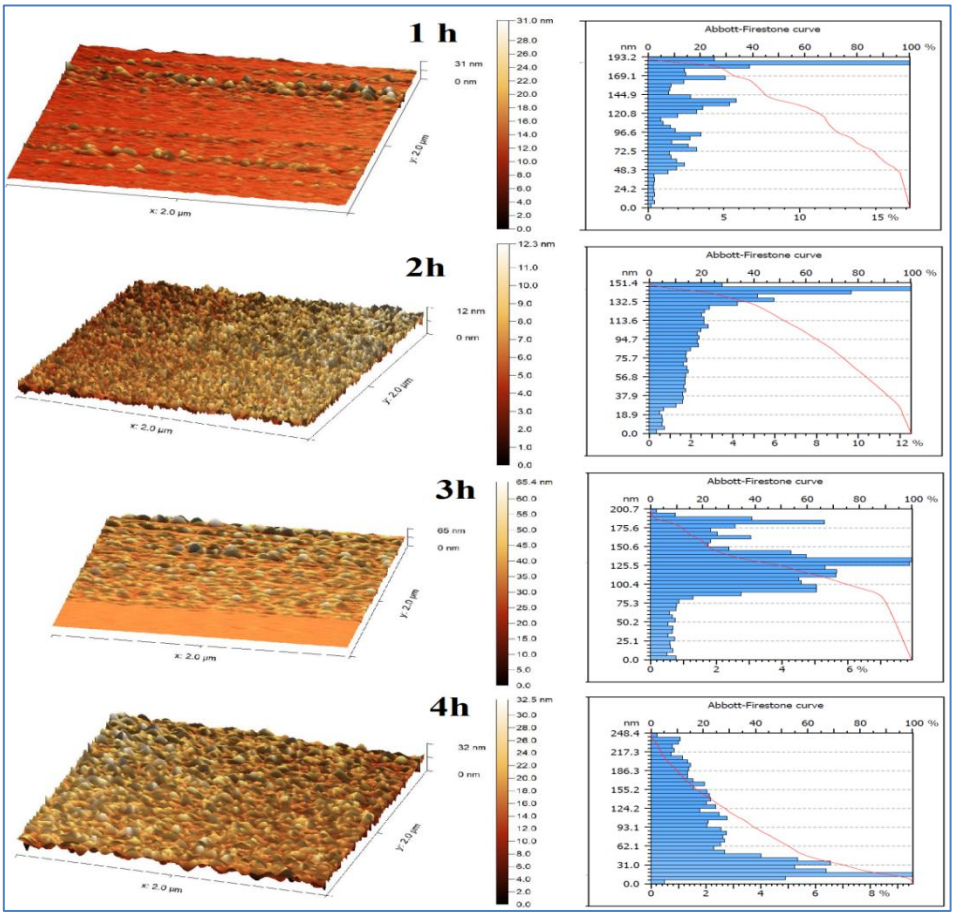

Fig. 3: AFM images and particle grain distribution of CdTe thin films deposited at different immersion times.

Table 2: AFM results of CdTe thin films deposited at different immersion times.

Deposition time (h)	Average diameter (nm)	Root mean square (RMS) Roughness (nm)
1	97.32	3.25
2	101.25	4.12
3	121.53	4.78
4	125.75	5.67

Figure 4 illustrates the FTIR transmittance spectra of the CdTe thin films deposited with different immersion times in the wavenumber range of 400-4000 cm-1. The FTIR spectrum showed significant vibrational bands at specific wavenumbers, corresponding to characteristic molecular vibrations in the sample. These bands provide a picture of atomic bonding and functional groups in the

DOI:https://doi.org/10.25130/tjps.v31i1.1875

prepared samples. The peak at (3445.77 cm^{-1}) is attributed to O-H stretching, indicating the presence of hydroxyl groups on the surface of the samples. While the band at (2075.05 cm^{-1}) indicates the bending vibration of the O-H bond, and the vibrational band at (1639 cm^{-1}) indicates the N-H stretching vibration, which indicates the presence of adsorbed groups from the atmosphere [29]. Several bands of intensity between (1466 and 1075 cm^{-1}) were observed due to the vibrations of the metal hydroxyl groups (Cd-OH). The broad peak at (701.86 cm^{-1}) confirms the formation of the CdTe structure to form the bond between Cd^{2+} and Te^{2+} ions [30]. The slight shift in the FTIR bands reveals structural changes induced by varying deposition time. We notice a decrease in the bond energy at (701.86 cm^{-1}), which indicates an increase in the bond length, and this result is consistent with the results of XRD [31].

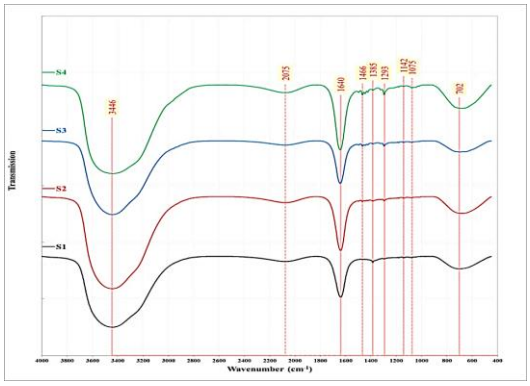

Fig. 4: FTIR spectra of CdTe thin films deposited at different immersion times: S1= 1h, S2= 2h, S3= 3h, and S4= 4h.

Table 3: Bonds in the FTIR spectrum of CdTe thin films deposited at different immersion times.

Deposition time	1 h	2 h	3 h	4 h
-OH	3445.77	3445.77	3443.30	3448.25
O-H bending	2075.05	2077.53	2075.05	2082.47
N-H stretching	1639.59	1639.59	1639.59	1642.06
Cd-OH	-	1466.39	1466.39	1466.39
	1384.74	1384.74	1389.69	1387.22
	1293.30	1293.20	1293.40	1293.10
	1142.27	1142.11	1142.33	1147.22
	1075.46	1074.22	1073.21	1072.99
Cd-Te	701.86	691.96	687.33	682.06

Figure 5 shows the UV-Vis absorbance curves of CdTe thin films prepared with different immersion times. In general, for all prepared samples, the absorbance decreases with increasing wavelength, because only photons with energy greater than the energy gap can interact with the material and form electron-hole pairs. The overall absorbance increases with increasing deposition time. This behaviour occurs because increasing the deposition time increases the thickness, potentially affecting the absorption properties. In addition, the edge sharpness increases with increasing deposition time, indicating improved crystallization and the removal of crystalline defects, as shown by the XRD results. Furthermore, the absorption edge shifts slightly towards longer wavelengths (a red shift), indicating a decrease in the energy gap—this shift assignment shows how deposition time affects the electronic structure of the prepared films.

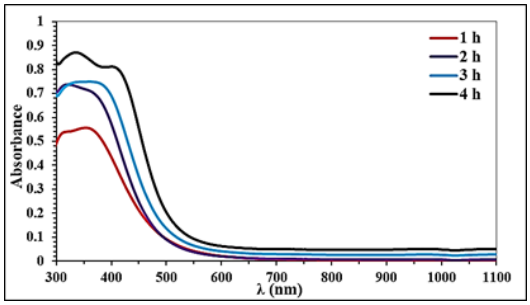

Fig. 5: UV-Vis absorption spectrum of CdTe thin films deposited at different immersion times

The absorption coefficient (α) of CdTe thin films deposited at different immersion times is shown in

DOI:https://doi.org/10.25130/tjps.v31i1.1875

Figure 6. The figure shows a high absorption coefficient (>10^4 cm^-1), especially at short wavelengths. This value indicates a direct electronic transition, as shown by previous studies. [32]. The increasing absorption coefficient with immersion time results from a red shift of the absorption edge, indicating a narrowing of the energy gap. The probability of generating an electron-hole pair is higher because less energy is required. A high absorption coefficient indicates that photons are absorbed more efficiently, making it suitable for applications that require direct electronic transitions, such as solar cells.

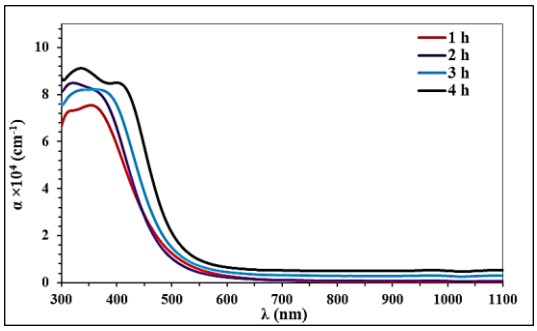

Fig. 6: Absorption coefficient of CdTe thin films deposited at different immersion times.

The optical band gap ($E_g^{Opt.}$The optical band gap of the nano-CdTe film samples was determined utilizing Tauc's plot of (αhυ)2 versus photon energy (hυ) as shown in Figure 7. The energy gap values decrease from (2.82 eV) to (2.62 eV) with increasing deposition time from (1 to 4 h) as a result of increasing the crystallite size, as shown by XRD results, as listed in Table 4. The results indicate that the electronic structure changes with increasing particle size, with the energy gap related to the nanoparticles' size according to the quantum confinement principle. Smaller particles have more confined electronic states, so it requires more energy to excite an electron. Such changes significantly affect the sample's optical and electrical properties, making it suitable for a wide range of applications. [33].

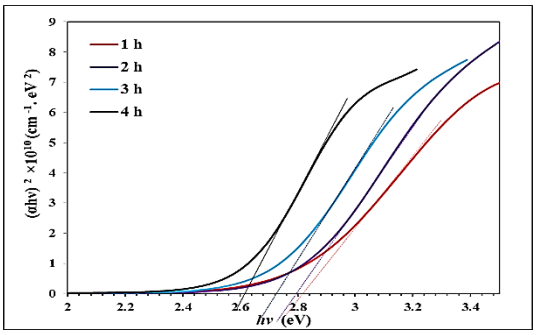

Fig. 7: Optical energy gap of CdTe thin films deposited at different immersion times.

Figure 8 shows the variation of the extinction coefficient (k) over the wavelength range (300-1100 nm) for CdTe thin films deposited at different immersion times. The k values indicate how strongly the material absorbs light and are mainly determined by the absorption coefficient; they therefore exhibit similar behavior, with maximum values in the absorption range and increasing with increasing deposition time.

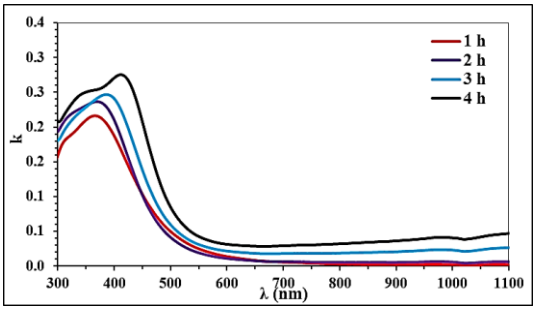

Fig. 8: Variation of the extinction coefficient of the prepared thin films.

Figure 9 shows the refractive index (n) spectra for CdTe thin films deposited with different immersion times. The refractive index at the absorption edge increases slightly with increasing deposition time, reflecting enhanced crystallinity. The refractive index mainly depends on the degree of crystallinity of the samples. Grain boundaries in polycrystalline materials act as sources of light scattering. The nanostructure and particle packing also play important roles in altering the refractive index. [34].

DOI:https://doi.org/10.25130/tjps.v31i1.1875

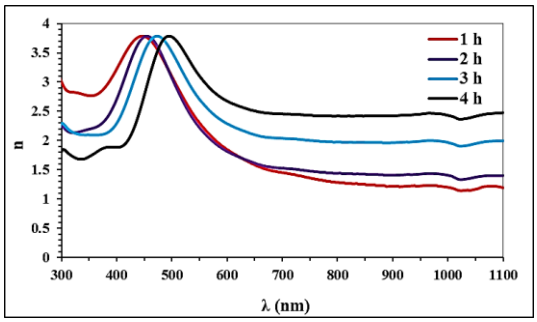

Fig. 9: Variation of refractive index with wavelength for CdTe thin films deposited with different immersion times

Figure 10 shows the spectra of the real dielectric constant in the range of (300-1100 nm) for CdTe thin films deposited with different immersion times. The real dielectric constant depends primarily on the refractive index and shows almost the same behaviour. Figure 11 shows the spectra of the imaginary dielectric constant of CdTe thin films deposited at different immersion times. These parameters are very important in understanding the properties of light and its interaction with materials, and are used in many photovoltaic applications. [35].

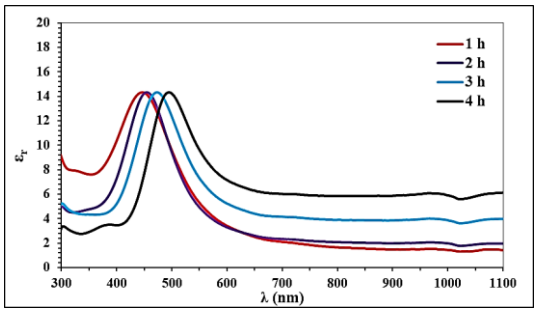

Fig. 10: Real dielectric constant of CdTe thin films deposited at different immersion times.

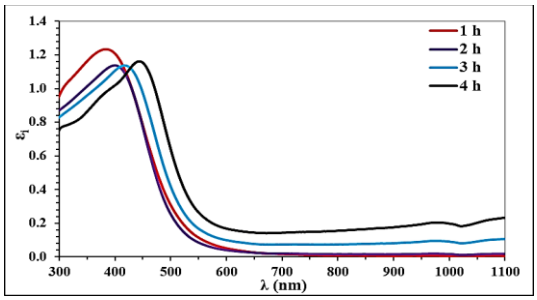

Fig. 11: Imaginary dielectric constant of CdTe films deposited at different immersion times.

Table 4 shows the values of optical parameters, including transmittance (T), absorption coefficient (α), extinction coefficient (k), refractive index (n), dielectric constants at (500 nm), as it is nearly the optimal intensity of the solar spectrum, and energy gap of CdTe thin films deposited at different immersion times. The transmittance values of the first sample were found to be (38 %), while they decreased to (12.14 %) at a deposition time of (4 h).

Table 4: Optical constants at (500 nm) wavelength for CdTe thin films deposited at different immersion times.

Time (h)	T (%)	α (cm^{-1})	K	n	ε_r	ε_i	E_g (eV)
1	38.43	12500	0.050	3.095	9.575	0.308	2.85
2	39.22	10400	0.041	3.071	9.427	0.254	2.80
3	24.35	14949	0.060	3.513	12.340	0.418	2.70
4	12.14	21296	0.085	3.773	14.230	0.640	2.60

CONCLUSIONS

This study investigated the effects of varying immersion periods in CdTe nanoparticle suspensions, prepared via pulsed laser, on the structural and optical properties of deposited thin films. XRD analysis revealed a polycrystalline structure with improved crystallinity and an increase in crystallite size with increasing immersion time. AFM analysis showed that longer immersion times led to increased particle diameter and surface roughness. The optical absorbance of the films increased, and the energy band gap narrowed slightly with increasing deposition time. FTIR confirmed the formation of the CdTe structure. These observed changes enhance the thin films' potential for optoelectronic applications, such

DOI:https://doi.org/10.25130/tjps.v31i1.1875

as radiation detectors.

Conflict of interests: The authors declare that there is no conflict of interest regarding the publication of this paper.

Sources of funding: This research did not receive any specific grant from funding agencies in the public, commercial, or not-for-profit sectors.

Author contributions: The authors contributed equally to this study.

REFERENCES

1. Kumar H, Singh M. Consequences of Post-Annealing on Optical, Structural and Electrical Properties of Cadmium Telluride Thin Films for Solar Cells Applications. Int J Thin Fil Sci Tec. 2025;14(1):21-6. https://doi.org/10.18576/ijtfst/140104

2. Jamwal D, Mehta SK. Metal Telluride Nanomaterials: Facile Synthesis, Properties and Applications for Third Generation Devices. ChemistrySelect. 2019;4(6):1943-63. https://doi.org/10.1002/slct.201803680.

3. Mouhammed AA, Saleh AN. Simulation Effect of Ga2O3 layer thickness on CdTe solar cell by SCAPS-1D. Tikrit Journal of Pure Science. 2019;24(6):110-6. https://doi.org/10.25130/j.v24i6.895

4. Salih, A. I. (2019). Optical dispersion characterization of CZTS thin films prepared by sol-gel at different annealing temperatures. Tikrit Journal of Pure Science, 24(7), 82-88.

5. de Melo O. Introduction to II-VI semiconductors. Handbook of II-VI Semiconductor-Based Sensors and Radiation Detectors: Volume 1, Materials and Technology: Springer; 2023. p. 3-19. https://doi.org/10.1007/978-3-031-19531-0_1.

6. Salih, A. R. (2024). Optimal Winter and Summer Settings of Solar Photovoltaic Panels for Many Locations in the World. Tikrit Journal of Pure Science, 29, 6.

7. Nayef UM, Muayad MW, Noori AS, Hadi AJ. Synthesis of zinc oxide nanoparticles via laser ablation on porous silicon for gas sensor applications. Journal of Optics. 2025:1-15. https://doi.org/10.1007/s12596-025-02531-y

8. Kadim AM. Applications of cadmium telluride (CdTe) in nanotechnology. Nanomaterials-Toxicity, Human Health and Environment: IntechOpen; 2019. https://doi.org/10.5772/intechopen.85506

9. Sultan RB, Al Suny A, Hossain MH, Noor T, Chowdhury MH. Particle swarm optimization for performance enhancement of cadmium telluride thin film solar cells by embedded nano-grating structures with a plasmonic metal coating layer. Heliyon. 2024;10(19). https://doi.org/10.1016/j.heliyon.2024.e38775.

10. Mostafa AM. The Influence of Various Parameters on the Ablation and Deposition Mechanisms in Pulsed Laser Deposition. Plasmonics. 2025:1-19. https://doi.org/10.1007/s11468-024-02706-6

11. Veleschuk V, Vlasenko O, Vlasenko Z, Gnatyuk V, Levytskyi S. Dependence of the CdTe melting threshold on the pulse duration and wavelength of laser radiation and the parameters of non-equilibrium charge carriers. Ukrainian journal of physics. 2017(62,№ 2):159-65. https://doi.org/10.15407/ujpe62.02.0159.

12. Singh R, Soni R. Laser-induced heating synthesis of hybrid nanoparticles. Noble Metal-Metal Oxide Hybrid Nanoparticles: Elsevier; 2019. p. 195-238. https://doi.org/10.1016/B978-0-12-814134-2.00011-5.

13. Nyabadza A, McCarthy É, Makhesana M, Heidarinassab S, Plouze A, Vazquez M, et al. A review of physical, chemical and biological synthesis methods of bimetallic nanoparticles and applications in sensing, water treatment, biomedicine, catalysis and hydrogen storage. Advances in colloid and interface science. 2023;321:103010. https://doi.org/10.1016/j.cis.2023.103010.

14. Harif MN, Rahman KS, Rosly HN, Chelvanathan P, Doroody C, Misran H, et al. An approach to alternative post-deposition treatment in CdTe thin films for solar cell applications.

Superlattices and Microstructures. 2020; 147: 106687. https://doi.org/10.1016/j.spmi.2020.106687.

15. Chander S, Purohit A, Lal C, Dhaka M. Enhancement of optical and structural properties of vacuum evaporated CdTe thin films. Materials Chemistry and Physics. 2017;185:202-9. https://doi.org/10.1016/j.matchemphys.2016.10.024.

16. Khrypunov G, Romeo A, Kurdesau F, Bätzner D, Zogg H, Tiwari AN. Recent developments in evaporated CdTe solar cells. Solar energy materials and solar cells. 2006;90(6):664-77. https://doi.org/10.1016/j.solmat.2005.04.003.

17. Pathok HS, Adhyapak S, Boruah M, Das AK, Saikia PK. The Influence of Deposition Time on the Structural, Morphological, and Optical Properties of Cdmns Thin Films. Morphological and Optical Properties of CdMn Thin Films. https://doi.org/10.2139/ssrn.4976607.

18. Najm A, Naeem HS, Majdi HS, Hasbullah SA, Hasan HA, Sopian K, et al. An in-depth analysis of the nucleation and growth mechanism of CdS thin film synthesized by the chemical bath deposition (CBD) technique. Scientific Reports. 2022;12(1):15295. https://doi.org/10.1038/s41598-022-19340-z.

19. Saxena N, Kumar P, Gupta V, Kanjilal D. Radiation stability of CBD-grown nanocrystalline CdS films against ion beam irradiation for solar cell applications. Journal of Materials Science: Materials in Electronics. 2018;29:11013-9. https://doi.org/10.1007/s10854-018-9183-0.

20. Daud MNM, Zakaria A, Jafari A, Ghazali MSM, Abdullah WRW, Zainal Z. Characterization of CdTe films deposited at various bath temperatures and concentrations using electrophoretic deposition. International journal of molecular sciences. 2012;13(5):5706-14. https://doi.org/10.3390/ijms13055706.

21. Manivannan V, Enzenroth RA, Barth KL, Kohli S, McCurdy PR, Sampath WS. Microstructural features of cadmium telluride photovoltaic thin film devices. Thin Solid Films. 2008;516(6):1209-13. https://doi.org/10.1016/j.tsf.2007.05.043.

22. Arce-Plaza A, Sánchez-Rodríguez F, Courel-Piedrahita M, Galán OV, Hernández-Calderón V, Ramírez-Velasco S, et al. CdTe thin films: deposition techniques and applications. Coatings and Thin-Film Technologies. 2018:131-48. https://doi.org/10.5772/intechopen.79578.

23. Wegner K, Piseri P, Tafreshi HV, Milani P. Cluster beam deposition: a tool for nanoscale science and technology. Journal of Physics D: Applied Physics. 2006;39(22):R439. https://doi.org/10.1088/0022-3727/39/22/R02.

24. Patil PC, Gaikwad AA, Phase V, Kadam R, Shirsath SE, Chamargore JJ. Rare earth Ce and Y cation co-substitution and its effects on the strain, elasticity, and magnetism of Co-Zn ferrite nanomaterials. Ceramics International. 2025. https://doi.org/10.1016/j.ceramint.2025.02.329

25. Salman MO, Kadhim MA, Khalefa AA. CdO: SnO2 composite UV-Assisted room temperature ozone sensor. Iraqi Journal of Science. 2023:1190-202. https://doi.org/10.24996/ijs.2023.64.3.15.

26. Camacho-Espinosa E, Mis-Fernández R, Loeza-Poot M, Bartolo-Pérez P, Peña J. Band gap analysis for nanometric sputtered CdTe and CdS films. Materials Science and Engineering: B. 2024;303:117281. https://doi.org/10.1016/j.mseb.2024.117281.

27. Usharani K, Balu A. Structural, optical, and electrical properties of Zn-doped CdO thin films fabricated by a simplified spray pyrolysis technique. Acta Metallurgica Sinica (English Letters). 2015;28:64-71. https://doi.org/10.1007/s40195-014-0168-6.

28. Yang J-H, Yin W-J, Park J-S, Ma J, Wei S-H. Review of first-principles study of defect properties of CdTe as a solar cell absorber. Semiconductor Science and Technology. 2016;31(8):083002. https://doi.org/10.1088/0268-1242/31/8/083002.

29. Lalitha S, Sathyamoorthy R, Senthilarasu S, Subbarayan A, Natarajan K. Characterization of CdTe thin film—dependence of structural and optical properties on temperature and thickness.

Solar energy materials and solar cells. 2004;82(1-2):187-99. https://doi.org/10.1016/j.solmat.2004.01.017.

30. Ranjbarzadeh S, Omid H, Razmara N. Facile One-Pot Solvothermal Synthesis of Nanocrystalline CdTe with Different Shapes. Int J Nanoparticles Nanotech. 2019;5:023. https://doi.org/10.35840/2631-5084/5523.

31. Junaid M, Batoo KM, Hussain SG, Khan WQ, Hussain S. Photodegradation of CdTe thin film via PVD for water splitting to generate hydrogen energy. Results in Chemistry. 2023;6:101102. https://doi.org/10.1016/j.rechem.2023.101102.

32. da Costa P, Merízio LG, Wolff N, Terraschke H, de Camargo ASS. Real-time monitoring of CdTe quantum dots growth in aqueous solution. Scientific Reports. 2024;14(1):7884. https://doi.org/10.1038/s41598-024-57810-8.

33. Cheng P, Wei X, Dai Z, Zhang Y, Yang Y, Liu J, et al. Tunable electronic and optical properties of CdO/ZrS2 heterostructure based on first principles. Chemical Physics. 2025:112654. https://doi.org/10.1016/j.chemphys.2025.112654

34. Hai HTN, Nguyen TT, Nishibori M, Ishihara T, Edalati K. Photoreforming of plastic waste into valuable products and hydrogen using a high-entropy oxynitride with distorted atomic-scale structure. Applied Catalysis B: Environment and Energy. 2025;365:124968. https://doi.org/10.1016/j.apcatb.2024.124968

35. Hértilli S, Yahyaoui N, Zeiri N, Baser P, Said M, Saadaoui S. Theoretical modeling of nonlinear optical properties in spheroidal CdTe/ZnTe core/shell quantum dot embedded in various dielectric matrices. Results in Physics. 2024;56:107274. https://doi.org/10.1016/j.rinp.2023.107274.